REGULAR ARTICLE

blood advances

Monocytes in leukapheresis products affect the outcome of CD19–targeted CAR T-cell therapy in patients with lymphoma

Cristiana Carniti,[1,*] Nicole M. Caldarelli,[1,2,*] Luca Agnelli,[3,4] Tommaso Torelli,[3,4] Silva Ljevar,[5] Sadhana Jonnalagadda,[1] Giada Zanirato,[1] Eugenio Fardella,[1,2] Federico Stella,[1,2] Daniele Lorenzini,[3] Silvia Brich,[3] Flavio Arienti,[6] Anna Dodero,[1] Annalisa Chiappella,[1] Martina Magni,[1,†] and Paolo Corradini[1,2,†]

[1]Hematology Division, Fondazione IRCCS Istituto Nazionale dei Tumori, Milan, Italy; [2]School of Medicine, Università degli Studi di Milano, Milan, Italy; [3]Department of Diagnostic Innovation, [4]Department of Molecular Oncology 1, [5]Biostatistics for Clinical Research Unit, and [6]Service of Immunohematology & Transfusion Medicine, Fondazione IRCCS Istituto Nazionale dei Tumori, Milan, Italy

Key Points

- Combining circulating absolute monocyte count and a 4-gene monocyte signature at leukapheresis predicts PFS of LBCL receiving CAR T cells.
- Monocytes depletion from apheresis products could result in improved outcome of patients with R/R LBCL receiving CD19–directed CAR T cells.

CD19–directed chimeric antigen receptor (CAR) T cells can induce durable remissions in relapsed/refractory large B-cell lymphomas (R/R LBCLs), but 60% of patients do not respond or relapse. Biological mechanisms explaining lack of response are emerging, but they are largely unsuccessful in predicting disease response at the patient level. Additionally, to maximize the cost-effectiveness of CAR T-cell therapy, biomarkers able to predict response and survival before CAR T-cell manufacturing would be desirable. We performed transcriptomic and functional evaluations of leukapheresis products in 95 patients with R/R LBCL enrolled in a prospective observational study, to identify correlates of response and survival to tisagenlecleucel and axicabtagene ciloleucel. A signature composed of 4 myeloid genes expressed by T cells isolated from leukapheresis products is able to identify patients with a very short progression-free survival (PFS), highlighting the impact of monocytes in CAR T-cell therapy response. Accordingly, response and PFS were also negatively influenced by high circulating absolute monocyte counts at the time of leukapheresis. The combined evaluation of peripheral blood monocytes at the time of leukapheresis and the 4-gene signature represents a novel tool to identify patients with R/R LBCL at very high risk of progression after CAR T-cell therapy and could be used to plan trials evaluating CAR T cells vs other novel treatments or allogeneic CAR T cells. However, it also highlights the need to incorporate monocyte depletion strategies for better CAR T production.

Introduction

CD19–directed chimeric antigen receptor (CAR) T-cell therapy has shown high efficacy, and tisagenlecleucel (tisa-cel) and axicabtagene ciloleucel (axi-cel) became the standard-of-care for relapsed/refractory large B-cell lymphomas (R/R LBCLs) in Italy. However, only 40% of patients experience durable remissions and the determinants of treatment failures are still inconsistently defined.[1]

Submitted 2 January 2024; accepted 3 February 2024; prepublished online on *Blood Advances* First Edition 15 February 2024; final version published online 15 April 2024. https://doi.org/10.1182/bloodadvances.2024012563.

*C.C. and N.M.C. contributed equally to this study.

†M.M. and P.C. contributed equally to this study.

NanoString expression data of this article are publicly available on the NCBI Gene Expression Omnibus database (accession number GSE243973).

Data generated in this study are available on request from the corresponding authors, Paolo Corradini (paolo.corradini@unimi.it), Cristiana Carniti (cristiana.carniti@istitutotumori.mi.it), and Luca Agnelli (luca.agnelli@istitutotumori.mi.it).

The full-text version of this article contains a data supplement.

To date, the majority of parameters used to predict CAR T-cell therapy success, including bridging therapy success, tumor burden at infusion, and CAR T-cell in vivo expansion,[2-13] are generated at the time of or after CAR T-cell infusion. However, to maximize the cost-effectiveness of CAR T-cell therapy, biomarkers able to predict response and survival before CAR T-cell manufacturing, are urgently required.

The generation of anti-CD19 CAR T cells with optimal expansion potential and effector activity could also depend on pre-manufacturing T-cell characteristics. In fact, this was demonstrated for patients with chronic lymphocytic leukemia receiving CTL019 therapy, where sustained remission was associated with an elevated frequency of $CD8^+$ T cells with memory-like features collected at the time of leukapheresis.[14] However, data on the composition of leukapheresis products of patients with LBCL treated with commercial anti-CD19 CAR T cells in relation to clinical efficacy are still lacking.

To identify biomarkers capable of predicting response before CAR T manufacturing, we conducted a single center prospective observational study and dissected T-cell phenotypic and transcriptomic properties of leukapheresis products obtained from patients with LBCL receiving tisa-cel or axi-cel and performed correlative analysis.

Methods

Study design and patients

This single center, observational study included 95 patients with R/R LBCL who received standard-of-care tisa-cel or axi-cel between December 2019 and January 2023. The study (INT180/19) was approved by the ethics committee, conducted in accordance with the Declaration of Helsinki, and involved patients who provided written informed consent. Patient characteristics and clinical outcomes are summarized in supplemental Tables 1 and 2. Patients who achieved complete response or partial response by day 90, as per Lugano 2014 classification,[15] assessed by computed tomography scan and positron emission tomography–computed tomography scan, were considered responders. Patients with stable disease or progressive disease and patients who died due to progression were considered nonresponders.

nCounter gene expression assay

Gene expression was measured on NanoString nCounter Analysis System (NanoString Technologies) using the nCounter 780 gene CAR T-cell characterization panel (XT-CSO-HCART1-12).

Cryopreserved leukapheresis products and leftover donor lymphocyte infusions (healthy controls) were rapidly thawed and subjected to $CD3^+$ T-cell separation on the auto-MACS separator using anti-CD3 microbeads (all from Miltenyi Biotec). Total RNA was extracted from $CD3^+$ T cells using the miRNeasy Mini Kit (Qiagen). The yield and quality of RNA were assessed using NanoDrop ND-1000 Spectrophotometer (NanoDrop Technologies) and the TapeStation 4200 (Agilent). One hundred nanogram of total RNA was used as input and hybridization was performed according to manufacturer's instructions. Detailed information on data analysis is reported in supplemental Methods.

Flow cytometry immunophenotyping

CAR T cells were longitudinally monitored in peripheral blood (PB) through multiparameter flow cytometry (MFC) using CD19 CAR detection reagent, as previously described,[11] or CD19 CAR FMC63 Idiotype (REA1297) (both from Miltenyi Biotec). CAR T-cell differentiation in infusion product leftovers was assessed by MFC as previously described.[11] Antibodies and gating strategies are detailed in supplemental Material. Data were acquired on BD FACSCanto II (BD Biosciences), MACSQuant Analyzer MQ10 or MQ16 (Miltenyi Biotec) and analyzed using FlowJo-v10 and MACSQuantify softwares.

Identification of lymphocyte-monocyte complexes with DEPArray platform

To visualize lymphocyte-monocyte complexes with the DEPArray (Menarini-Silicon Biosystems), thawed leukapheresis samples were stained with CD3-PE (REA613) and CD14-APC (REA599) antibodies (Miltenyi Biotec), fixed using flow cytometry fixation buffer (R&D Systems) and counterstained with 4',6-diamidino-2-phenylindole (DAPI) solution (Merck Millipore).

Statistical analyses

Time of CAR T-cell administration was used as origin in all time-to-event analyses. Kaplan-Meier estimate with the log-rank test was used for survival curves. For group comparison of categorical data, $\chi 2$ test was used. Spearman correlation test was used to compare continuous variables, with the exception of the comparison between NanoString expression and quantitative reverse transcription polymerase chain reaction (qRT-PCR) data, where Kendall's tau was used to limit biases due to the occurrence of null values. Student *t* test, Mann-Whitney, or Kruskal-Wallis tests were used to assess differences among distributions. All reported *P* values are 2-sided and are statistically significant when $P < .05$. Plots and statistical analysis were performed with R software v4.1.2 and GraphPad Prism v.9.00.

The association of variables with progression-free survival (PFS) was studied using univariable and multivariable Cox models. The association of variables with the response at 90 days was studied using univariable and multivariable logistic models, where the absence of response was considered as an event. The reported odds ratios (ORs) >1 thus indicate the risk of nonresponse. Nonlinear effect of continuous numerical variables was estimated using restrictive cubic splines with 3 knots positioned at the quartiles. The variables used to generate multivariable models were selected based on their significance in univariable analysis, with the exclusion of redundant and linked parameters. The nested Cox and logistic models were confronted using the likelihood ratio test. The improved significance of the 4-gene model in multivariate analysis was assessed as previously described.[16]

Results

A 4-gene signature in leukapheresis T cells segregates patients with different survival outcomes.

To address the potential effect of T-cell phenotypes before CAR T-cell manufacturing on the outcome of 95 patients with LBCL treated with tisa-cel and axi-cel, we examined T-cell subsets in leukapheresis products (n = 67) using MFC. No difference in the

frequencies of T naïve (T_N), T stem cell memory (T_{SCM}), T central memory (T_{CM}), T effector memory (T_{EM}), and T effector (T_E) subsets among $CD4^+$ and $CD8^+$ T cells were observed in patients stratified according to clinical baseline features (supplemental Figure 1; supplemental Tables 3-6). Only age above the median (55 years) was associated to decreased CD4+T_N and CD8+T_N cells ($P < .0001$ and $P < .001$, respectively; supplemental Table 7). Contrary to day 90 response, which was affected by levels of CD8 T cells ($P < .05$; supplemental Table 8), high CAR T-cell expansion in vivo, which is essential for response and survival (supplemental Figure 2A-D; Monfrini et al[11]), was linked to higher frequencies of T_{SCM} in leukapheresis products (supplemental Table 9; supplemental Figure 2E). Patients with CAR^+ cells per μL at day 10 (C_{10}) above the median value (expanders) showed higher levels of CD8+T_{SCM} cells ($P < .05$; supplemental Table 9) and frequencies of these cells were positively correlated with those of CAR+CD8+T_{CM} in infusion products (IPs; Spearman correlation = 0.3; $P < .05$). The latter population in IPs was relevant for CAR T-cell in vivo expansion and efficacy ($P < .05$; supplemental Figure 2F), as already shown.[11]

We next interrogated the transcriptional profile of T cells contained in leukapheresis products of 77 patients, whose clinical characteristics are similar to those of the entire study cohort (supplemental Table 10) and identified a 4-gene transcriptional signature (including *MS4A4A, CD86, CD163,* and *SIGLEC5*) able to divide patients into 2 groups, from now on called 4-gene signature positive (SIG^{pos}) and 4-gene signature negative (SIG^{neg}) respectively, characterized by significantly different survival probabilities (Figure 1A-B). SIG^{pos} have shorter PFS (median PFS for SIG^{pos} was 61 days and not reached for SIG^{neg}, $P < .0001$; Figure 1B) and the expression of the 4 genes also identifies patients more frequently refractory to CAR T cells (stable or progressive diseases at day 90 [supplemental File]). Notably, the expression of the 4 genes was associated with the phenotype of CAR T cells in IPs and with CAR T-cell in vivo expansion capabilities but did not differ when patients were stratified according to the infusion product they received (SIG^{pos}: tisa-cel, 41% and axi-cel, 59%; SIG^{neg}: tisa-cel, 49% and axi-cel, 51%; OR, 0.7153; χ^2 test 95% confidence interval [CI], 0.2889-1.732; P = not significant [ns]). SIG^{pos} exhibited lower frequencies of CAR+CD8+T_{CM} ($P < .01$; Figure 1C) and lower circulating CAR T-cell levels when compared to SIG^{neg} patients ($P < .01$; Figure 1D). Of note, the expression of the 4-gene signature did not correlate with the occurrence of either cytokine release syndrome (any grade: 75% for SIG^{pos} vs 76% for SIG^{neg} [OR, 0.9706; χ^2 test 95% CI, 0.3604-2.950; P = ns]) or immune-effector-cell–associated neurotoxicity syndrome (any grade: 19% for SIG^{pos} vs 18% for SIG^{neg} [OR, 1.005; χ^2 test 95% CI, 0.3159-3.411; P = ns]). These results establish a link between transcriptional features of T cells contained in leukapheresis products, CAR T-cell product properties, and CAR T-cell expansion in vivo, which are known to contribute to patient response and survival.

The robustness of the 4-gene model in predicting survival was confirmed using a leave-one-out and linear discriminant analysis as crossvalidation procedure and prediction method, respectively (supplemental File, section survival analysis "LOOCV based on LDA"). To further evaluate the efficiency of the model, we randomly stratified the cohort into unbiased training and test group, obtaining complete overall accuracy (supplemental File, section survival analysis "Testing models").

To validate the 4-gene signature, 24 additional samples were profiled by NanoString. The addition of these samples to the original cohort retained the model significance as shown by the 101 sample heat map and Kaplan-Meier analysis (supplemental Figure 3; supplemental File, section survival analysis "4-gene model evaluation in extended 101 sample cohort").

For clinical implementation, we compared the nCounter expression data with those obtained by qRT-PCR using TaqMan-based assays specific for the 4 genes of interest (supplemental Figure 4A-D). A highly significant correlation between the expression levels was established, thus warranting qRT-PCR as a simple and reliable tool to stratify patients in the 2 prognostic risk groups (supplemental Figure 4E-H), even when we minimized the number of assays to 3 (supplemental File, section "PCR validation").

The gene signature is the result of monocyte–T cell complexes present in leukapheresis products

Surprisingly, the 4 genes contained in the signature are highly expressed in monocytes but not in T cells. MS4A4A is selectively expressed by monocytes, tissue resident macrophages, and tumor-associated macrophages (TAM) as it is induced during monocyte-to-macrophage differentiation and polarization toward a M2/M2-like direction.[17] CD86 is expressed on monocytes and its binding to CTLA-4 inhibits the lymphocyte activation.[18,19] CD163 is exclusively expressed on monocytes/macrophages[20] and its expression in TAM is a strong indicator of poor prognosis in several cancers,[21-23] possibly due to the inhibition of T-cell activation.[24,25] Over expression of SIGLEC5 on monocytes could impair $CD8^+$ proliferation and induce T-cell exhaustion.[26] These literature data prompted us to question whether monocytes contained in leukapheresis products had a role in determining the outcome of patients with LBCL treated with CAR Ts and if they did, what that role was.

First, to understand why we had detected a monocyte profile while examining $CD3^+$ selected cells, we interrogated flow cytometry data acquired before CD3 cell separation and found that patients overexpressing the 4 genes had significantly higher levels of monocytes in their leukapheresis products ($P = .01$; Figure 2A). More importantly, a subpopulation within unsorted and sorted CD3+T cells, stained positive for both CD3 and CD14 (Figure 2B) and the proportion of these double positive events was higher in SIG^{pos} ($P < .001$; Figure 2C). These events were not MFC artifacts but complexes of 2 cells or sometimes even 3 cells containing at least 1 monocyte cell expressing CD14 and 1 or 2 lymphocyte cells expressing CD3, as shown by the visualization using the DEPArray PLUS image-based platform (Figure 2D). Of note, levels of monocytes and complexes did not differ in tisa-cel and axi-cel products (not shown).

The nature of the T cells contained in the complexes was further analyzed: frequencies of different T-cell subsets found in complexes reflected the relative abundance of each T-cell subset in leukapheresis products (supplemental Figure 5A-B). Additionally, SIG^{pos} have increased levels of all T-cell subset:monocyte complexes when compared with those in SIG^{neg}, mirroring the fact that SIG^{pos} have collectively more complexes (supplemental Figure 5C-F) and supporting the hypothesis that the inferior survival of SIG^{pos} could be due to higher frequencies of suppressive monocytes in their leukapheresis products.

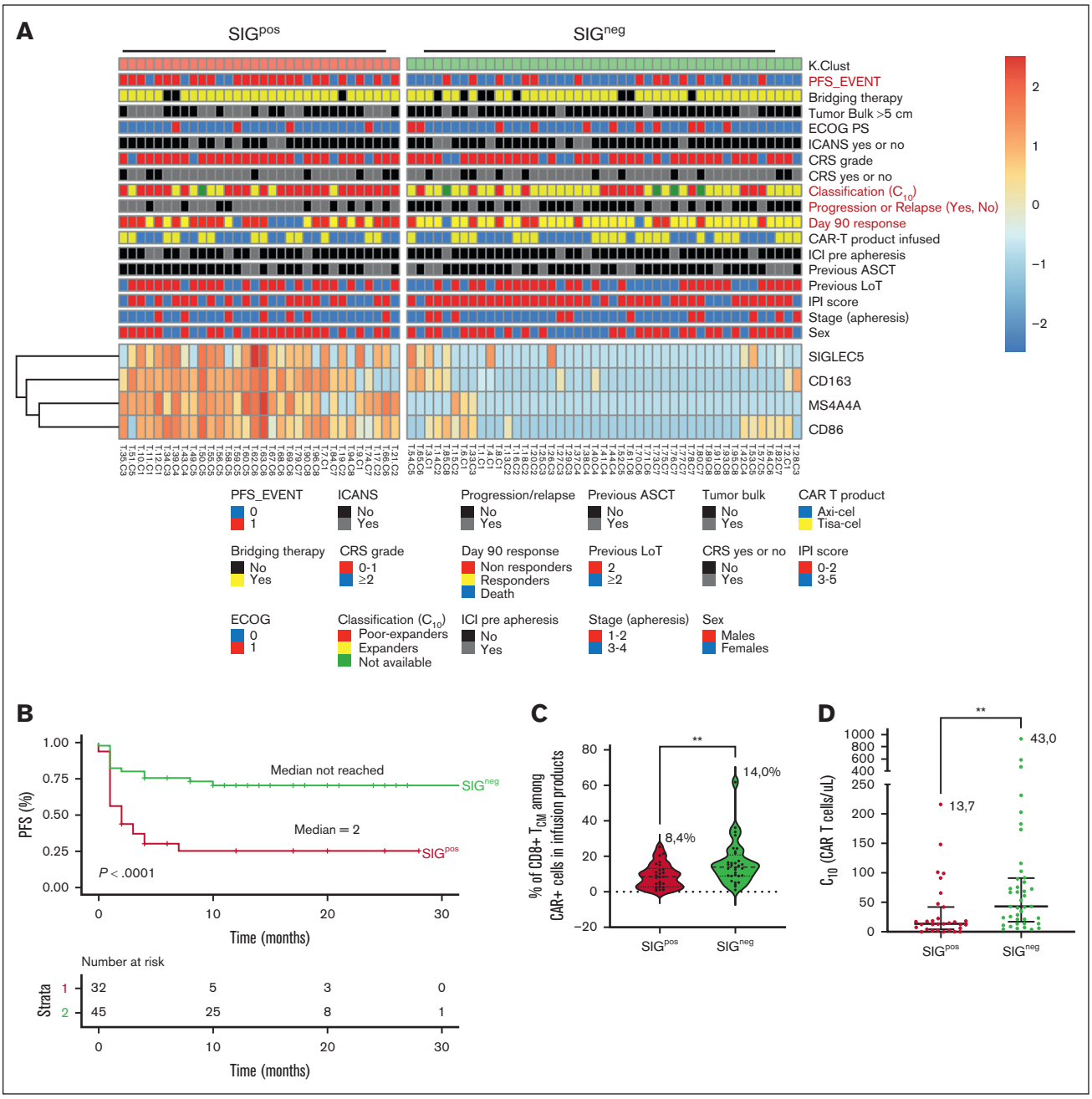

Figure 1. A 4-gene signature in leukapheresis products correlate with survival of patients with lymphoma receiving CAR T-cell therapy. (A) Heat map clustering of patients based on the expression of the 4 genes in $CD3^+$ selected cells (n = 77). After separation, median $CD3^+$ population purity was 98.2%. Ward and Canberra were used as linkage and distance metrics, respectively. Patients' features are shown alongside the code (ASCT, CRS, classification C_{10}, ECOG, ICANS, ICI, IPI, LoT, and PFS). (B) Kaplan-Meier estimate of PFS in patients stratified according to the 4-gene model (n = 77). SIG^{pos}, 4-gene signature positive (group 1), SIG^{neg}, 4-gene signature negative (group 2). (C) Percentage of CAR+CD8+T_{CM} cells in IPs of SIG^{pos} and SIG^{neg} (n = 58). (D) Concentration of CAR T cells at day 10 after infusion (C_{10}) in SIG^{pos} and SIG^{neg} (n = 72). In panels C-D, exact median values are reported, Mann-Whitney test was used for comparisons. $^{**}P < .01$. ASCT, autologous stem cell transplantation; CRS, cytokine release syndrome; classification C_{10}, classification of expanders and poor-expanders patients according to the number of circulating CAR T cells at day 10 after infusion (C_{10}, patients were dichotomized into expanders and poor-expanders using the median C10 as cutoff); ECOG, Eastern Cooperative Oncology Group performance status; ICANS, immune-effector-cell–associated neurotoxicity syndrome; ICI, immune checkpoint inhibitors; IPI, international prognostic index; LoT, lines of therapies before leukapheresis.

Of note, these lymphocyte-monocyte complexes were also present in leukapheresis products of 4 patients with mantle cell lymphoma receiving brexucabtagene autoleucel, 2 patients with multiple myeloma receiving ciltacabtagene autoleucel, and in 8 healthy controls (donor lymphocyte infusions) (supplemental Figure 6). Nonetheless, the 4 genes were only expressed at

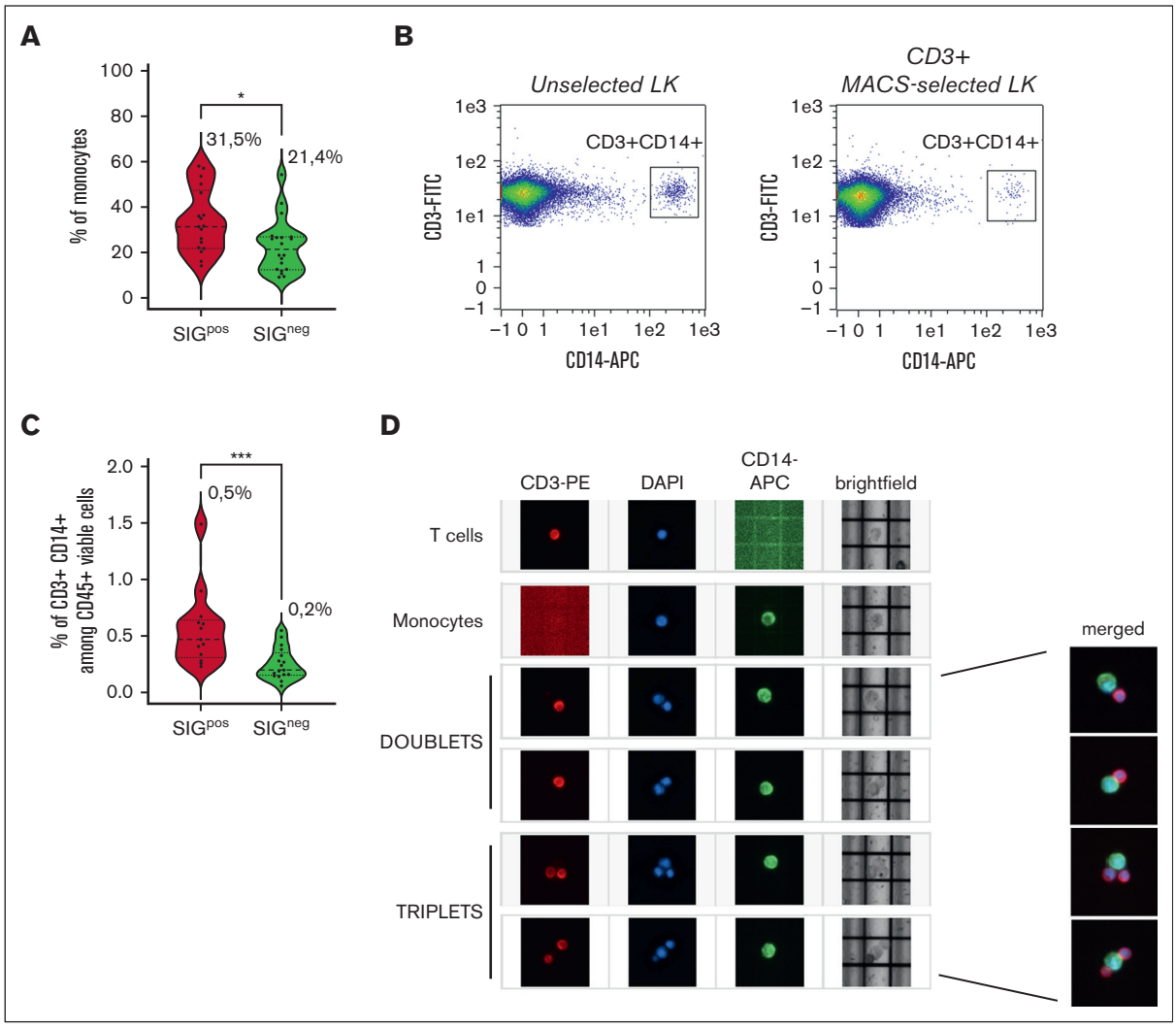

Figure 2. The myeloid gene signature is related to the presence of lymphocyte-monocyte complexes in LKs. (A) Frequency of monocytes evaluated by flow cytometry in the LKs of patients expressing the 4-gene signature (SIG^{pos}) or not (SIG^{neg}), n = 38. (B) Representative density plots showing $CD3^+$ and $CD14^+$ cells (among singlets, viable, and $CD3^+$ cells), in an unselected LK (left) and in a MACS-selected $CD3^+$ selected LK (right). (C) Percentage of $CD3^+$ $CD14^+$ cells, evaluated by MFC, among $CD45^+$ viable cells in unsorted LKs of SIG^{pos} and SIG^{neg} (n = 30). (D) Random gallery of events for $CD3^+$ T cells, $CD14^+$ monocytes, and doublets/triplets expressing both CD3 and CD14, in unsorted LKs visualized using DEPArray PLUS image-based platform. 4′,6-diamidino-2-phenylindole (DAPI) was used to stain nuclei. Experiments were performed using samples belonging to 3 different patients. Exact median values are reported. In panels A and C, comparisons were made by the Mann-Whitney test (*$P < .05$; ***$P < .001$). LK, leukapheresis product.

high levels in the subset of LBCL characterized by poor PFS, whereas no expression was detected in healthy controls (supplemental File, section survival analysis, "Heat map of genes correlated with PFS") or in patients with multiple myeloma or mantle cell lymphoma (not shown), suggesting the specific role of the signature in determining the prognosis of patients with LBCL.

Response and survival are negatively influenced by high circulating absolute monocyte levels in an inflammatory microenvironment

In line with the fact that SIG^{pos} had higher frequencies of monocytes in leukapheresis products by MFC (Figure 2A), we confirmed the presence of elevated monocytes at cell count both in leukapheresis products ($P < .01$) and PB obtained at the time of leukapheresis ($P < .05$), together with a significant decrease in lymphocytes both in leukapheresis products ($P < .01$) and in PB ($P < .05$), resulting in a low lymphocyte-monocyte ratio in SIG^{pos} ($P < .001$) (supplemental Figure 7A-L).

We then checked whether monocyte levels could influence response and survival to CAR T-cell therapy. Univariate analysis indicated that among parameters predicting relapse,[4,9] levels of LDH, C-reactive protein (CRP), and ferritin at the time of infusion, in vivo CAR-T expansion, are all covariates associated with response at day 90 and PFS, whereas response to bridging therapy was significantly associated with survival only (supplemental Tables 11 and 12). On the other hand, when considering parameters at leukapheresis, percentages of lymphocytes in

leukapheresis products and in PB, percentages of monocytes in leukapheresis products, and absolute monocyte counts (AMC) in leukapheresis products and in PB, together with CRP levels, significantly affected response and survival (supplemental Tables 13 and 14). In particular, nonresponders had higher AMC in leukapheresis products ($P < .01$), higher percentages of monocytes ($P < .01$), but also decreased percentages of lymphocytes ($P < .001$), and lower ratios of lymphocytes and monocytes ($P < .001$; Figure 3A-F). Moreover, consistent with the fact that frequencies and absolute monocyte PB counts significantly correlated with those in leukapheresis products (Spearman r = 0.4744, $P < .0001$ and $r = 0.6621$, $P < .0001$), nonresponders also had significantly higher circulating AMC ($P < .001$) and lower frequencies of lymphocytes ($P < .05$; Figure 3G-L) at the time of leukapheresis but not at infusion after lymphodepletion. The reduced presence of circulating lymphocytes at the time of leukapheresis in nonresponder patients confirm literature data reporting that patients with low PB $CD3^+$ cell counts at leukapheresis are characterized by shorter PFS.[27]

Of interest, PB AMC levels at leukapheresis were not influenced by clinical parameters (supplemental Figure 8A-H). On the other hand, systemic inflammation assessed by CRP and ferritin levels was associated with increased circulating AMC. Patients with serum CRP and ferritin levels higher than the upper limit of normal had significantly higher AMC ($P < .01$ for CRP at leukapheresis; $P < .001$ for CRP at infusion; $P < .05$ for ferritin at infusion) (supplemental Figure 8I-K). Additionally, higher levels of CRP, LDH, and ferritin were associated with the expression of the signature (supplemental Figure 9A-E), thus suggesting that an inflammatory microenvironment and high monocytes levels coexist in patients characterized by 4-gene signature and could contribute to determining an inferior outcome.

In accordance with this, both a random forest analysis run to assess variable importance (supplemental File, section survival analysis "Test variables against PFS" and "Test variable against D90 response") and multivariate analysis confirmed that response to bridging therapy and in vivo CAR-T expansion significantly affected survival ($P = .0317$ and $P = .0085$, respectively), together with PB AMC levels at the time of leukapheresis ($P = .0202$; supplemental Figure 10A; supplemental Table 15). Disease response was influenced by in vivo CAR-T expansion ($P = .0068$), ferritin levels ($P = .0098$), and PB AMC levels at the time of leukapheresis ($P = .0169$) (supplemental Figure 10B; supplemental Table 16). Importantly, when the impact of the 4-gene signature was tested in the multivariate model, the monocyte signature together with PB AMC levels and response to bridging therapy outperformed in vivo CAR-T expansion in predicting PFS (likelihood ratio test between 2 models, $P = .0068$ [Figure 4; supplemental Tables 17 and 18]) and all these variables were also associated with response together with ferritin levels (likelihood ratio test between 2 models, $P = .0176$ [supplemental Figure 11A-B; supplemental Tables 19 and 20]).

The combination of high circulating AMC and the monocyte signature identifies an increased proportion of patients at high risk of progression

Because predicting the success of CAR T-cell therapy before manufacturing might be crucial for patients and health care sustainability, we next verified if we could identify patients at high risk of progression by evaluating parameters assessable at the time of leukapheresis. Remarkably, although high CRP levels, the percentage of lymphocytes in PB and monocyte counts in PB are all associated with significantly reduced survival (supplemental Table 14), the shortest PFS was achieved when patients expressing the 4-gene signature and displaying monocyte counts above the median were selected. Namely, median PFS for SIG^{pos} with high monocyte counts was 32.5 days vs 209 days for SIG^{pos} with low monocytes ($P < .05$; Figure 5A). Of note, also the selection of patients with high CRP levels and expressing the 4-gene signature, identifies a group with very short median PFS despite not significantly reduced when compared to that of patients characterized by the expression of the signature and a less inflamed systemic microenvironment (median PFS for SIG^{pos} with high CRP was 37 days vs 209 days for SIG^{pos} with low CRP [P = ns; Figure 5B]). Median PFS for SIG^{pos} with low percentage lymphocytes was also particularly short, 48.5 days vs 209 days for SIG^{pos} with high percentage of lymphocytes (P = ns). These findings strongly support the hypothesis that the poor outcome of some patients with LBCL receiving CAR T-cell therapy may be attributed to the presence of high monocytes levels expressing the 4-gene signature.

Higher frequencies of $CD14^{hi}$ monocytes coexpressing MS4A4A, CD86, CD163, and SIGLEC5, are associated with the monocyte signature and disease response

To characterize monocytes in bulk leukapheresis products, we analyzed the distribution of the 3 different monocyte populations defined by CD14 and CD16 expression: classical (cMo,$CD14^{hi}CD16^{neg}$), intermediate (iMo,$CD14^{hi}CD16^{pos}$), and nonclassical monocytes (ncMo,$CD14^{low}CD16^{pos}$).[28] We detected a numerical increase of iMo in SIG^{pos} when compared to SIG^{neg} ($P < .05$), whereas frequencies of cMo and ncMo were largely comparable (supplemental Figure 12A-B), but no difference was found stratifying patients on response (supplemental Figure 12C). We then investigated the monocyte activation patterns using C-C motif chemokine receptor 2 (CCR2) surface marker. Consistent with recently reported data in healthy individuals,[29,30] CCR2 was preferentially expressed on cMo and less on iMo (cMo median 88.1% [range, 76.61%-99.15%] vs iMo median 42.2% [range, 18.89%-65.84%]), whereas there was almost no expression on ncMo (median 0.92% [range, 0.17%-6.59%]). Notably, the percentage of iMo CCR2 positive was significantly higher in SIG^{pos} ($P < .01$; supplemental Figure 12D), possibly indicating an increased propensity of monocytes for trafficking and macrophage polarization in SIG^{pos}.

We next evaluated whether the protein expression of MS4A4A, CD86, CD163, and SIGLEC5 in leukapheresis products could identify a population of monocytes differentially present in SIG^{pos} vs SIG^{neg}. Concatenated monocyte fluorescent data from 30 patients, analyzed with FlowSOM, a clustering-based algorithm, revealed the presence of a metacluster characterized by the expression of all 4 proteins (Figure 6A), mainly consisting of $CD14^{hi}$ monocytes when visualized on a t-SNE (t-stochastic neighbor embedding) map (Figure 6B-C). This population was significantly more represented in SIG^{pos} ($P < .05$; Figure 6D) and was enriched in nonresponders ($P < .05$; Figure 6E).

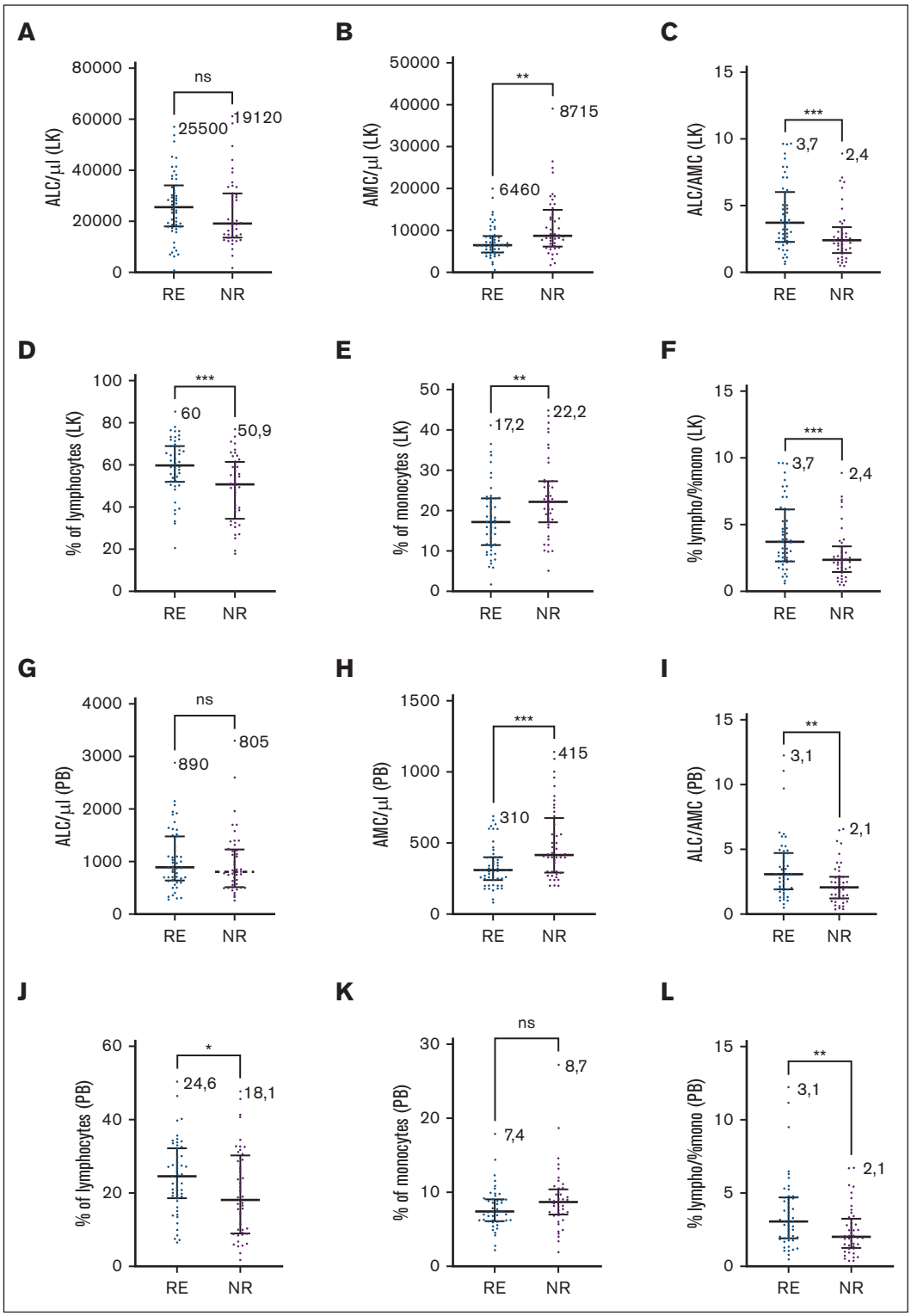

Figure 3. Absolute counts and percentages of lymphocytes and monocytes in LK and in PB at the time of leukapheresis are different in RE and NR. (A) ALC in LK of RE = 51 and NR = 44 at day 90 after CAR T-cell infusion. (B) AMC in LK of RE and NR. (C) ALC/AMC ratio in LK of RE and NR. (D) Percentage of lymphocytes in LK of RE and NR. (E) Percentage of monocytes in LK of RE and NR. (F) Lymphocytes/monocytes (%) ratio in LK of RE and NR. (G) ALC in PB at the time of LK (PB) of RE and NR. (H) AMC in PB of RE and NR. (I) ALC/AMC ratio in PB of RE and NR. (J) Percentage of lymphocytes in PB of RE and NR. (K) Percentage of monocytes in PB of RE and NR. (L) Lymphocytes/monocytes (%) ratio in PB of RE and NR. In panels A-L, data of 95 patients were analyzed. In panels A-L, data refer to peripheral absolute blood count the day of LK or absolute cell count in LK products, exact median values are reported. *P* values were calculated applying the Mann-Whitney test. ns, not significant; **P* < .05; ***P* < .01; ****P* < .001. ALC, absolute lymphocyte count; LK, leukapheresis products; NR, nonresponders; RE, responders.

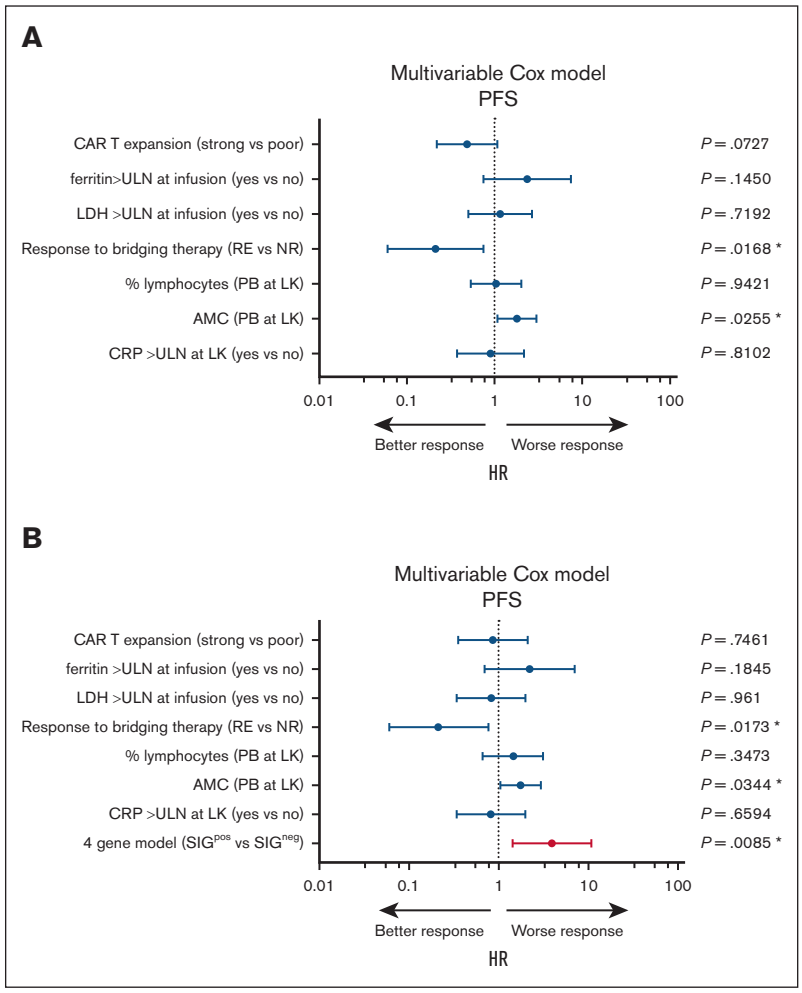

Figure 4. The 4-gene model predicts survival in multivariate analysis. (A) Forest plot showing results of multivariate Cox regression model assessing potential clinical and biological risk factors for PFS. The analysis was performed in 65 patients. Compared with supplemental Figure 10A, the numerosity was lowered due to missing values in the "4-genes model" variable shown in panel B. (B) Forest plot showing results of multivariate Cox regression model assessing potential clinical and biological risk factors for PFS, with the addition of the 4-gene model. The analysis was performed in 65 patients. The nested Cox models were compared using the likelihood ratio test. *P* value of the addition of the variable "4 gene model" = .0068.

The relevance of protein expression of MS4A4A, CD86, CD163, and SIGLEC5 on monocytes in bulk apheresis products was then assessed in 48 additional leukapheresis products. Even in these samples, using FlowSOM, we identified the presence of a metacluster expressing all 4 markers (supplemental Figure 13A) that, when visualized on the t-SNE maps (supplemental Figure 13B), seems to represent a discrete population of monocytes enriched within the classical and intermediate subtypes (supplemental Figure 13C). The levels of this population were significantly higher in nonresponders (supplemental Figure 13D), and when an analysis by receiver operating characteristic curve was performed to identify a specific level of MS4A4A+CD86+ CD163+SIGLEC5+ monocytes associated with response, a cutoff of 12% was identified, above which PFS was significantly reduced (log-rank test, $P = .01$; supplemental Figure 13E). These results further confirm the idea that the outcome of patients with LBCL treated with CAR T-cell therapy is affected by the presence of monocytes expressing the 4-gene signature. Importantly, flow cytometry data confirm that $CD3^+$ cells did not express the 4 proteins (supplemental Figure 14).

To validate the T suppressive functions of monocytes in leukapheresis products, given the impossibility of detecting a single population of monocytes expressing all the 4 proteins by conventional MFC precluding its sorting, we used a coculture in vitro system of sorted cMo, iMo, and ncMo from leukapheresis products and CAR^+ cells isolated from infusion bag left overs (n = 3 patients). A significant reduction in CD69 levels, a well-established activation marker of T cells, was detected on CAR T cells cocultured with $CD14^{hi}$ monocytes (encompassing cMo and iMo) (supplemental Figure 12E), suggesting a direct effect of $CD14^{hi}$ monocytes on T-cell functions. Importantly, monocytes form complexes with CAR T cells in vivo, and at the time of maximal CAR T-cell expansion, poor-expanders displayed higher levels of monocyte–CAR T-cell complexes, reinforcing the concept that monocytes affect CAR T-cell functionality (supplemental Figure 12F).

Of note, neither monocytic (Mo) nor polymorphonucler-myeloid-derived suppressor cells (MDSCs) frequencies were significantly different in leukapheresis products of SIG^{pos} compared to SIG^{neg} (supplemental Figure 15A-C), and their levels did not impact response at day 90 (supplemental Figure 15D-E).

Discussion

CAR T-cell therapy revolutionized treatment of patients with R/R LBCL and are moving fast toward earlier lines of treatment despite the fact that they do not yield consistent results across all patients.

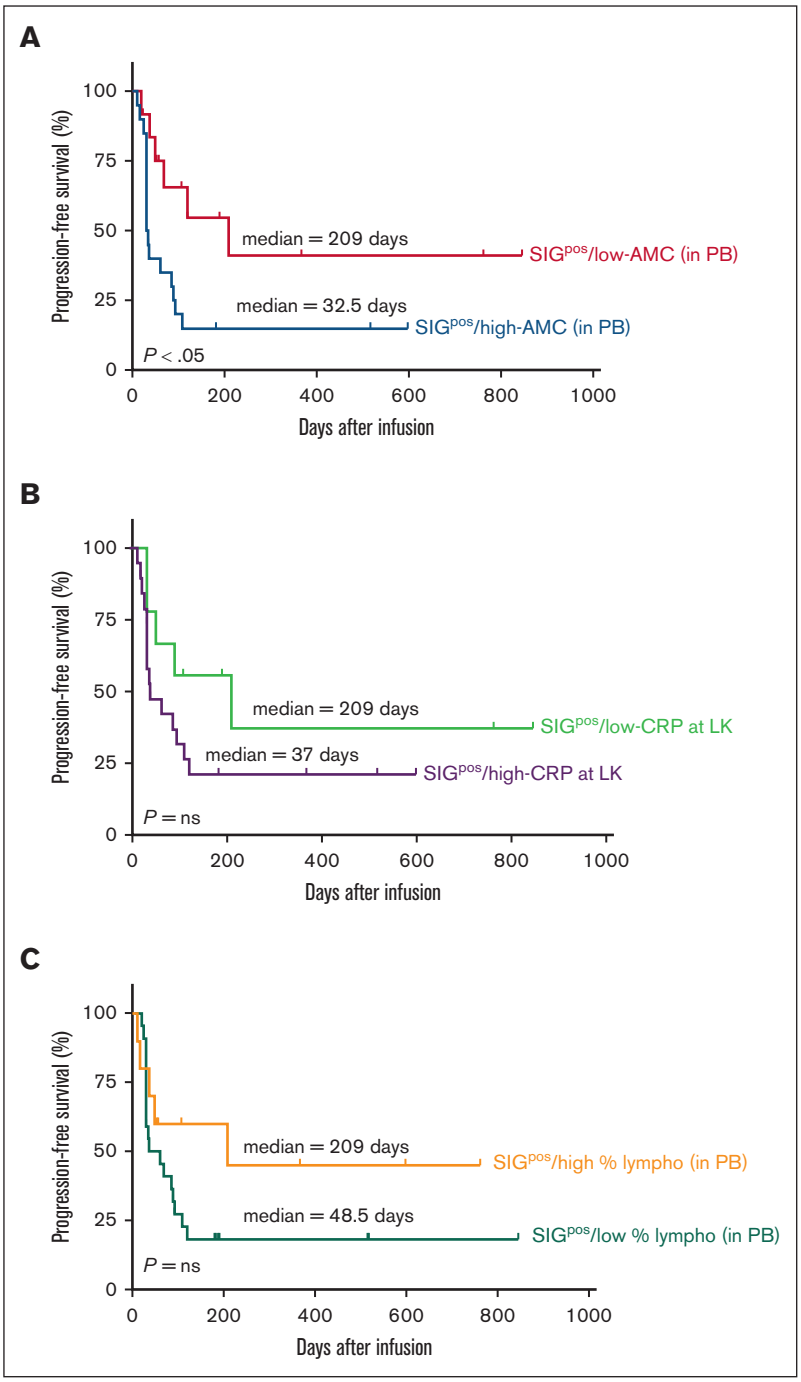

Figure 5. High levels of circulating AMC significantly reduced survival of patients expressing the signature. (A) Kaplan-Meier curve of PFS in patients stratified according to PB AMC levels at the time of leukapheresis and to the 4-gene signature (n = 32). The median value of AMC (360/μL) was used to dichotomize patients. SIG^{pos}/high-AMC, patients expressing the signature and displaying circulating AMC above the median (n = 20). SIG^{pos}/low-AMC, patients expressing the signature and displaying circulating AMC below the median (n = 12). (B) Kaplan-Meier curve of PFS in patients stratified according to CRP levels at the time of LK and to the 4-gene signature (n = 28). CRP upper normal limit (ULN) was used to dichotomize patients. SIG^{pos}/high-CRP, patients expressing the signature and displaying CRP levels above the ULN (n = 19). SIG^{pos}/low-CRP, patients expressing the signature and displaying CRP levels below the ULN (n = 9). (C) Kaplan-Meier curve of PFS in patients stratified according to the percentage of circulating lymphocytes at the time of leukapheresis and to the 4-gene signature (n = 32). The median value of the percentage of lymphocytes (21.6%) was used to dichotomize patients. SIG^{pos}/high % lympho, patients expressing the signature and displaying lymphocytes levels above the median (n = 10). SIG^{pos}/low % lympho, patients expressing the signature and displaying lymphocytes levels below the median (n = 22). Comparisons were made applying the log-rank test.

It is crucial to find biomarkers to maximize the clinical benefit of CAR T-cell therapy at single-patient level to improve outcome and support the economic sustainability for health care systems. In the present work, we developed a novel model combining the enumeration of circulating monocytes and a monocyte gene signature in leukapheresis products, able to identify a proportion of patients at very high risk of progression when treated with tisa-cel or axi-cel.

Previous works suggested that quality of CAR T-cell IPs depends on the starting T-cell phenotypes,[14] but the majority of data have been generated in patients with acute lymphoblastic leukemia or chronic lymphocytic leukemia and little is known for LBCL. In this study, a moderate increase in CD8+T_{SCM} in leukapheresis products was correlated with higher levels of CAR+CD8+T_{CM} in IP and with consistent CAR T-cell expansion, suggesting that less differentiated T-cell subsets in the leukapheresis can enhance CAR T-cell activity. Nonetheless, better CAR T-cell therapy outcomes might also be linked to the underlying molecular and metabolic pathways that control diversification in T-cell responses. Thus, to better resolve T-cell heterogeneity in pre-manufacturing leukapheresis products, we analyzed T-cell

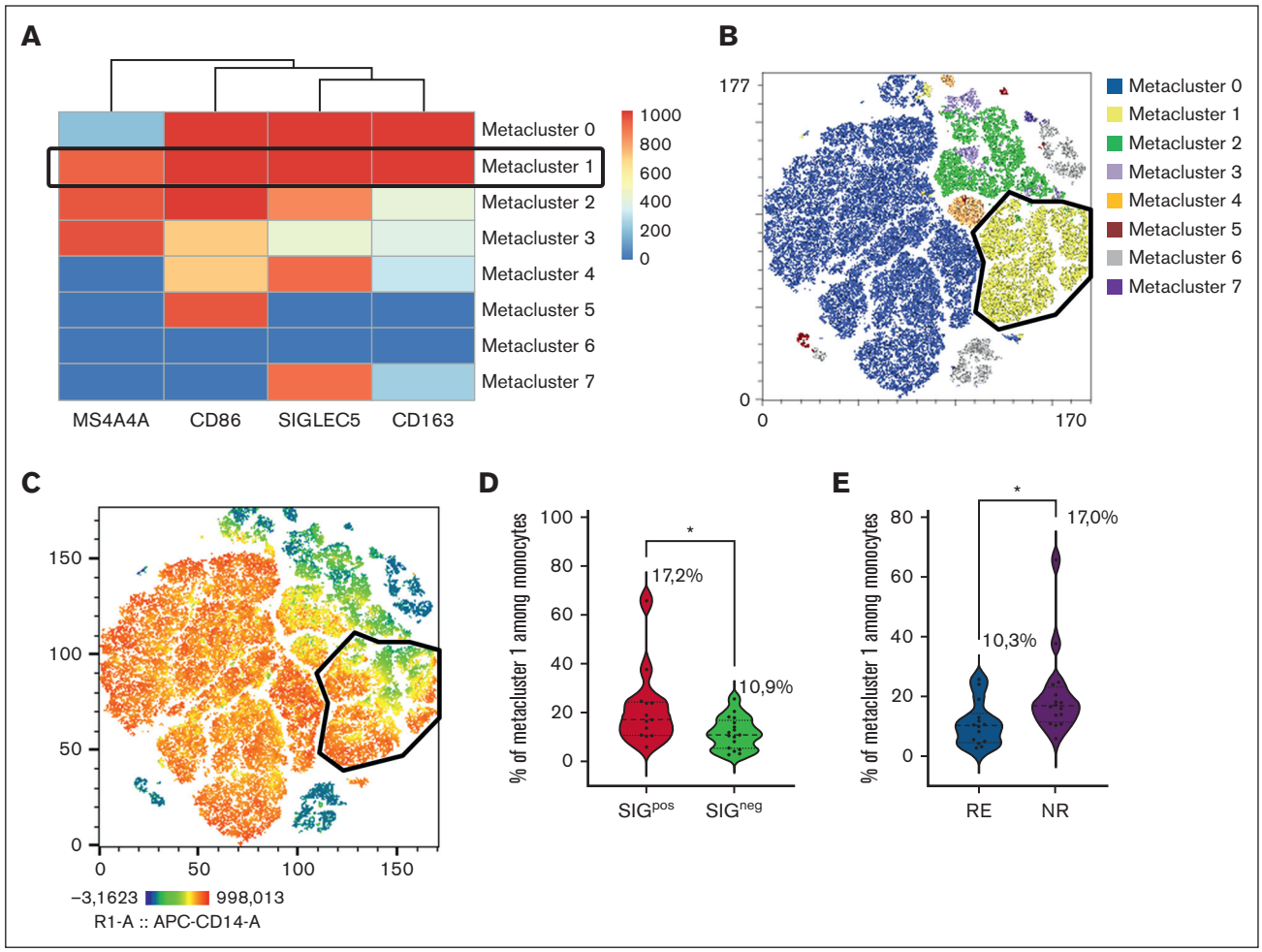

Figure 6. FlowSOM and t-SNE analyses pipelines identify a discrete population within CD14^{hi} monocytes coexpressing MS4A4A, CD86, SIGLEC5, and CD163 at the protein level in LKs. (A) Heat map visualization of marker expression in each of the 8 metaclusters generated by FlowSOM algorithm on concatenated monocytes data of 30 patients in bulk leukapheresis products (3000 cells per sample). The mean fluorescence intensity of each marker (MS4A4A, CD86, SIGLEC5, and CD163 columns) is displayed for each metacluster (rows), n = 30. (B) t-SNE, a nonlinear dimensionality reduction method, was used to visualize FlowSOM metaclusters. (C) t-SNE pseudocolored map representing expression of CD14 marker. Red indicates higher expression and blue indicates lower expression. (D) Percentage of metacluster 1 among monocytes in SIG^{pos} and SIG^{neg}. (E) Percentage of metacluster 1 among monocytes in RE and NR. In panels D-E, exact median values are reported. Comparisons were performed using Mann-Whitney test; *$P < .05$. FlowSOM, Flow Self-Organizing Map; t-SNE, t-distributed stochastic neighbor embedding.

features by transcriptomics and identified a highly significant correlation between the expression levels of 4 myeloid genes (*MS4A4A*, *CD86*, *CD163*, and *SIGLEC5*) and survival. The prognostic value of the gene signature proved to be robust, independently of the technique used (NanoString or RT-qPCR), thus demonstrating that RT-qPCR might become a fast and reproducible tool to stratify patients before CAR T-cell manufacturing.

The unexpected discovery of this group of monocyte-associated genes coexpressed by CD3+T cells allowed us to trace this signature to monocyte–T-cell complexes present in leukapheresis products, similar to what was described in the context of infectious diseases.[31,32] The frequency of these complexes was higher in patients expressing the signature and displaying shorter PFS, as was the frequency of monocytes in premanufacturing leukapheresis products, thus raising the question of whether monocytes can affect CAR T-cell efficacy along with supporting B-cell survival and proliferation as already shown.[33] Of note, as high monocyte contamination in leukapheresis products is known to affect transduction efficiency, CAR T-cell activation, and tumor killing ability during the manufacturing process;[34] the fact that leukapheresis products contain CD14+CD3+ complexes, raises concerns regarding the most appropriate method used for monocyte depletion. The commonly used positive selection of T cells might in fact result in extensive monocyte contamination and limited CAR T-cell product quality.

The prognostic relevance of total monocyte count has been described in large cohorts of patients with LBCL,[35] but the impact of monocytes on CAR T-cell therapies has not been systemically studied to date. Here, we show that patients overexpressing the monocyte signature have increased number of monocytes in PB and leukapheresis products and are

characterized by high CRP levels and lower frequencies CAR+CD8+T_{CM} in IPs, a key correlate of CAR T-cell in vivo expansion and disease response.[11] Remarkably, although high CRP levels and monocyte counts are both associated with significantly reduced survival, the combined presence of the gene signature and high circulating monocytes, identifies a group of patients at very high risk of relapse, thus supporting the hypothesis that the particularly poor outcome of some patients with LBCL receiving CAR T cells is because of the presence of high monocytes levels expressing the 4-gene signature in an inflammatory peripheral immune environment.

The remarkably poor PFS of patients with high AMC levels at leukapheresis and the expression 4-gene model, together with the fact that in multivariate analysis both these variables were strongly associated with reduced survival, prompted us to question whether a specific population of immunosuppressive monocytes in bulk leukapheresis products might affect CAR T-cell features and ultimately impact on patient outcome. In line with this, we observed at the protein level, a population of cells expressing $CD14^{hi}$ and MS4A4A, CD86, CD163, and SIGLEC5, was more abundant in the SIG^{pos} group and in nonresponders. Although further studies will be required to identify a cutoff value able to discriminate patients with different outcome probabilities, these data indicate that the 4-gene signature translates into the presence of a group of monocytes present in bulk leukapheresis products directly affecting CAR T-cell response in LBCL.

Furthermore, the analysis of monocyte subsets indicated that SIG^{pos} had increased CCR2 levels in $CD14^{hi}$ iMo compared with SIG^{neg}. CCR2 mediates the recruitment of blood monocytes to tumor tissues, resulting in high density of CD163+TAMs, which are known to affect survival of patients with diffuse LBCL who received standard first-line regimens.[36] Of interest, in contrast to other studies that have recently identified a link between circulating MDSCs and CAR T cells in patients with LBCL,[37,38] in our study, quantities of Mo-MDSCs assessed by MFC in leukapheresis products, are neither associated with the signature nor with the outcome. Nonetheless, it is well known that monocytes and Mo-MDSCs have many overlapping functions and phenotypic markers, thus whether Mo-MDSCs represent a terminally differentiated cell type rather than a cell state induced by cancer and other diseases, requires additional evidence.

In summary, we identified a model combining PB AMC and a monocyte signature in leukapheresis products that can be interrogated before CAR T-cell manufacturing, valuable not only in helping to prognosticate durable responses but also in predicting immunological failure and tailoring alternative therapies, including allogeneic CAR Ts or bispecific antibodies. In addition to yielding a predictive model, these findings, although based primarily on correlations between biomarkers evaluated at the time of T-cell apheresis and survival, suggest novel mechanisms for CAR T-cell resistance. In particular, this study defines the important role of the myeloid compartment in shaping immune response before CAR T-cell infusion in patients with LBCL, and underscore the use of monocyte depletion for CAR T-cell production and the possibility to incorporate inhibition of monocytes in combinatorial approaches aiming to enhance CAR T-cell efficacy.

Acknowledgments

The authors are grateful to the patients who participated and their caregivers, as well as the health care professionals, hospital staff, and clinical study coordinators for supporting this research. The authors acknowledge the assistance of Giulia Bertolini in performing DEPArray experiments and Arianna Rigamonti for multiparameter flow cytometry data analysis.

This work was supported by the Associazione Italiana Contro le Leucemie - Linfomi e Mieloma, European Union–Next Generation EU–NRRP M6C2–Investment 2.1 Enhancement and strengthening of biomedical research in the NHS (project #PNRR-MAD-2022-12376059 and #PNC-E3-2022-23683269-PNC-HLS-TA), the Italian Ministry of Health Ricerca Finalizzata 2019 (project #RF-2019-12370243), the Cancer Research UK (C355/A26819), Fundacion Cientifica de la Asociación Espanola Conra el Cancer, and Italian Association for Cancer Research under the Accelerator Award Program.

Authorship

Contributions: C.C. conceived the study, analyzed data, and wrote the manuscript; N.M.C. performed experiments, analyzed data, and wrote the manuscript; L.A. and T.T. analyzed NanoString data; S.L. developed univariate and multivariate models; S.J. and G.Z. performed experiments; E.F., F.S., D.L., A.D., and A.C. collected clinical data; F.A. supervised leukapheresis procedures; S.B. loaded the cartridges and scanned the samples on the NanoString; M.M. performed experiments, analyzed data, and wrote the manuscript; P.C. conceived the study, analyzed data, and wrote the manuscript; and all authors edited and approved the final manuscript.

Conflict-of-interest disclosure: C.C. had travel and accommodations paid by a for-profit health care company (Novartis) during the past 3 years. A.C. served the advisory boards for Celgene/Bristol Myers Squibb (BMS), Gilead Sciences, Ideogen, Roche, Secura Bio, and Takeda, and received honoraria for lectures/educational activities from AstraZeneca, Celgene/BMS, Clinigen, Gilead Sciences, Incyte, Janssen, Novartis, Roche, and Takeda. P.C. received honoraria paid by for-profit health care companies including AbbVie, ADC Therapeutics, Amgen, Celgene, Daiichi Sankyo, Gilead/Kite, GlaxoSmithKline, Incyte, Janssen, Kyowa Kirin, Nerviano Medical Science, Novartis, Roche, Sanofi, and Takeda (consulting, advisory role, or lecturer) during the past 3 years, and had travel and accommodations paid by for-profit health care companies, including Novartis, Janssen, Celgene, BMS, Takeda, Gilead/Kite, Amgen, and AbbVie during the past 3 years. The remaining authors declare no competing financial interests.

ORCID profiles: C.C., 0000-0003-1039-1757; N.M.C., 0009-0008-2536-5766; S.L., 0000-0002-1151-1477; S.J., 0009-0006-6491-2537; E.F., 0009-0007-0273-1316; A.C., 0000-0002-2977-0098; M.M., 0000-0001-9458-5836; P.C., 0000-0002-9186-1353.

Correspondence: Paolo Corradini, Fondazione IRCCS Istituto Nazionale dei Tumori, Medical Oncology and Hematology-Allogeneic BMT Unit, via Venezian 1, 20133 Milan, Italy; email: paolo.corradini@unimi.it; and Cristiana Carniti, Hematology Division,

Fondazione IRCCS Istituto Nazionale dei Tumori, via Venezian 1, 20133 Milan, Italy; email: cristiana.carniti@istitutotumori.mi.it; and Luca Agnelli, Department of Diagnostic Innovation and Department of Molecular Oncology 1, Fondazione IRCCS Istituto Nazionale dei Tumori, via Venezian 1, 20133 Milan, Italy; email: luca.agnelli@istitutotumori.mi.it.

References

1. Zhang X, Zhu L, Zhang H, Chen S, Xiao Y. CAR-T cell therapy in hematological malignancies: current opportunities and challenges. *Front Immunol*. 2022;13:927153.
2. Schuster SJ, Svoboda J, Chong EA, et al. Chimeric antigen receptor T cells in refractory B-cell lymphomas. *N Engl J Med*. 2017;377(26):2545-2554.
3. Schuster SJ, Bishop MR, Tam CS, et al. Tisagenlecleucel in adult relapsed or refractory diffuse large B-cell lymphoma. *N Engl J Med*. 2019;380(1):45-56.
4. Neelapu SS, Locke FL, Bartlett NL, et al. Axicabtagene ciloleucel CAR T-cell therapy in refractory large B-cell lymphoma. *N Engl J Med*. 2017;377(26):2531-2544.
5. Locke FL, Ghobadi A, Jacobson CA, et al. Long-term safety and activity of axicabtagene ciloleucel in refractory large B-cell lymphoma (ZUMA-1): a single-arm, multicentre, phase 1-2 trial. *Lancet Oncol*. 2019;20(1):31-42.
6. Nastoupil LJ, Jain MD, Feng L, et al. Standard-of-care axicabtagene ciloleucel for relapsed or refractory large B-cell lymphoma: results from the US lymphoma CAR T consortium. *J Clin Oncol*. 2020;38(27):3119-3128.
7. Jacobson CA, Hunter BD, Redd R, et al. Axicabtagene ciloleucel in the non-trial setting: outcomes and correlates of response, resistance, and toxicity. *J Clin Oncol*. 2020;38(27):3095-3106.
8. Dean EA, Mhaskar RS, Lu H, et al. High metabolic tumor volume is associated with decreased efficacy of axicabtagene ciloleucel in large B-cell lymphoma. *Blood Adv*. 2020;4(14):3268-3276.
9. Vercellino L, Di Blasi R, Kanoun S, et al. Predictive factors of early progression after CAR T-cell therapy in relapsed/refractory diffuse large B-cell lymphoma. *Blood Adv*. 2020;4(22):5607-5615.
10. Bethge WA, Martus P, Schmitt M, et al. GLA/DRST real-world outcome analysis of CAR T-cell therapies for large B-cell lymphoma in Germany. *Blood*. 2022;140(4):349-358.
11. Monfrini C, Stella F, Aragona V, et al. Phenotypic composition of commercial anti-CD19 CAR T cells affects in vivo expansion and disease response in patients with large B-cell lymphoma. *Clin Cancer Res*. 2022;28(15):3378-3386.
12. Roddie C, Neill L, Osborne W, et al. Effective bridging therapy can improve CD19 CAR-T outcomes while maintaining safety in patients with large B-cell lymphoma. *Blood Adv*. 2023;7(12):2872-2883.
13. Haradhvala NJ, Leick MB, Maurer K, et al. Distinct cellular dynamics associated with response to CAR-T therapy for refractory B cell lymphoma. *Nat Med*. 2022;28(9):1848-1859.
14. Fraietta JA, Lacey SF, Orlando EJ, et al. Determinants of response and resistance to CD19 chimeric antigen receptor (CAR) T cell therapy of chronic lymphocytic leukemia. *Nat Med*. 2018;24(5):563-571.
15. Cheson BD, Fisher RI, Barrington SF, et al. Recommendations for initial evaluation, staging, and response assessment of Hodgkin and non-Hodgkin lymphoma: the Lugano Classification. *J Clin Oncol*. 2014;32(27):3059-3068.
16. Centonze G, Maisonneuve P, Simbolo M, et al. Lung carcinoid tumours: histology and Ki-67, the eternal rivalry. *Histopathology*. 2023;82(2):324-339.
17. Mattiola I, Mantovani A, Locati M. The tetraspan MS4A family in homeostasis, immunity, and disease. *Trends Immunol*. 2021;42(9):764-781.
18. Pinto BF, Medeiros NI, Teixeira-Carvalho A, et al. CD86 expression by monocytes influence an immunomodulatory profile in asymptomatic patients with chronic chagas disease. *Front Immunol*. 2018;9:454.
19. Souza PEA, Rocha MOC, Menezes CAS, et al. Trypanosoma cruzi infection induces differential modulation of costimulatory molecules and cytokines by monocytes and T cells from patients with indeterminate and cardiac Chagas' disease. *Infect Immun*. 2007;75(4):1886-1894.
20. Nguyen TT, Schwartz EJ, West RB, Warnke RA, Arber DA, Natkunam Y. Expression of CD163 (hemoglobin scavenger receptor) in normal tissues, lymphomas, carcinomas, and sarcomas is largely restricted to the monocyte/macrophage lineage. *Am J Surg Pathol*. 2005;29(5):617-624.
21. Jung KY, Cho SW, Kim YA, et al. Cancers with higher density of tumor-associated macrophages were associated with poor survival rates. *J Pathol Transl Med*. 2015;49(4):318-324.
22. Komohara Y, Jinushi M, Takeya M. Clinical significance of macrophage heterogeneity in human malignant tumors. *Cancer Sci*. 2014;105(1):1-8.
23. Park JY, Sung JY, Lee J, et al. Polarized CD163+ tumor-associated macrophages are associated with increased angiogenesis and CXCL12 expression in gastric cancer. *Clin Res Hepatol Gastroenterol*. 2016;40(3):357-365.
24. Liu S, Zhang C, Maimela NR, et al. Molecular and clinical characterization of CD163 expression via large-scale analysis in glioma. *Oncoimmunology*. 2019;8(7):1601478.
25. Etzerodt A, Tsalkitzi K, Maniecki M, et al. Specific targeting of CD163+ TAMs mobilizes inflammatory monocytes and promotes T cell–mediated tumor regression. *J Exp Med*. 2019;216(10):2394-2411.

26. Vuchkovska A, Glanville DG, Scurti GM, et al. Siglec-5 is an inhibitory immune checkpoint molecule for human T cells. *Immunology*. 2022;166(2):238-248.

27. Wada F, Jo T, Arai Y, et al. T-cell counts in peripheral blood at leukapheresis predict responses to subsequent CAR-T cell therapy. *Sci Rep*. 2022;12(1):18696.

28. Ziegler-Heitbrock L, Ancuta P, Crowe S, et al. Nomenclature of monocytes and dendritic cells in blood. *Blood*. 2010;116(16):e74-e80.

29. Auffray C, Sieweke MH, Geissmann F. Blood monocytes: development, heterogeneity, and relationship with dendritic cells. *Annu Rev Immunol*. 2009;27:669-692.

30. Wong KL, Tai JJY, Wong WC, et al. Gene expression profiling reveals the defining features of the classical, intermediate, and nonclassical human monocyte subsets. *Blood*. 2011;118(5):e16-e31.

31. Burel JG, Pomaznoy M, Lindestam Arlehamn CS, et al. The challenge of distinguishing cell-cell complexes from singlet cells in non-imaging flow cytometry and single-cell sorting. *Cytometry A*. 2020;97(11):1127-1135.

32. Burel JG, Pomaznoy M, Lindestam Arlehamn CS, et al. Circulating T cell-monocyte complexes are markers of immune perturbations. *Elife*. 2019;8:e46045.

33. Mueller CG, Boix C, Kwan W-H, et al. Critical role of monocytes to support normal B cell and diffuse large B cell lymphoma survival and proliferation. *J Leukoc Biol*. 2007;82(3):567-575.

34. Wang X, Borquez-Ojeda O, Stefanski J, et al. Depletion of high-content CD14+ cells from apheresis products is critical for successful transduction and expansion of CAR T cells during large-scale cGMP manufacturing. *Mol Ther Methods Clin Dev*. 2021;22:377-387.

35. Tadmor T, Bari A, Sacchi S, et al. Monocyte count at diagnosis is a prognostic parameter in diffuse large B-cell lymphoma: results from a large multicenter study involving 1191 patients in the pre- and post-rituximab era. *Haematologica*. 2014;99(1):125-130.

36. Li Y-L, Shi Z-H, Wang X, Gu K-S, Zhai Z-M. Tumor-associated macrophages predict prognosis in diffuse large B-cell lymphoma and correlation with peripheral absolute monocyte count. *BMC Cancer*. 2019;19(1):1049.

37. Jaeger U, Bishop MR, Salles G, et al. Myc expression and tumor-infiltrating T cells are associated with response in patients (Pts) with relapsed/refractory diffuse large B-cell lymphoma (r/r DLBCL) treated with tisagenlecleucel in the Juliet Trial. *Blood*. 2020;136(suppl 1):48-49.

38. Jain MD, Zhao H, Wang X, et al. Tumor interferon signaling and suppressive myeloid cells are associated with CAR T-cell failure in large B-cell lymphoma. *Blood*. 2021;137(19):2621-2633.